Photon drag current due to spin-flip transitions of electrons in nonsymmetric quantum wells

F. T. Vasko
Institute of Semiconductor Physics, NAS Ukraine, Kiev, 252650, Ukraine

O. Keller
Institute of Physics, Aalborg University, DK-9220 Aalborg Ost, Denmark
(Received 22 April 1998)

Photon drag current caused by transfer of momentum from absorbed far-infrared radiation to two-dimensional (2D) electrons is calculated for spin-flip transitions in nonsymmetric heterostructures. The induced current is not parallel to the longitudinal component of photon wave vector $\mathbf{q}$ because the contribution $[\mathbf{q}\times\mathbf{v}_s]$ ($\mathbf{v}_s$ is the characteristic spin velocity along the normal to 2D layer) is essential in the matrix element for spin-flip electron-photon interaction. Both spectral and angular dependencies of the current and the effect of the in-plane magnetic field are discussed for the short-range scattering case. Numerical estimations for typical parameters of InAs-based heterostructures and a THz pump with intensity 1 kW/cm^2 are presented.
[S0163-1829(98)04247-7]

I. INTRODUCTION

Photon drag (PD) current measurements are a specific tool for investigating the momentum-transfer kinetics under intersubband transitions in various systems (the intrasubband transitions are also studied in bulk *p*-type Ge). In the past decade PD currents have been studied for different kinds of two-dimensional (2D) electron systems (see Refs. 1 and 2). This kind of response is due to photon momentum transfer and different types of transitions are excited by such a dc current. The phenomenon may be interesting for development of a new type of ultrafast detectors also.[3] In connection with recent applications of intense THz radiation to study different types of electron responses in heterostructures (see Ref. 4 and references therein), the peculiarities of the PD currents for tunnel-coupled quantum wells (QWs) have been discussed in Refs. 5 and 6. In this paper we consider another system with closely spaced (with a few meV splitting energy corresponding THz spectral region) subbands: a nonsymmetric heterostructure in which the spin degeneration of the electron subbands is lifted.

While theoretical calculations of the spin-splitting of electron spectra in nonsymmetric heterostructures was started 20 years ago,[7–9] detailed experimental studies have been performed only recently. The measurements of Shubnikov–de Haas oscillations in different InAs-based heterostructures[10–13] demonstrate clearly a splitting energy of the order of a few meV for heavy-doped samples. Magneto-optical measurements permit to studies of the spin-splitting energy spectra in nonsymmetric GaAs-based QWs also.[14] Recent band-structure calculations[15,16] (using the $\mathbf{k}\cdot\mathbf{p}$ approach with corresponding boundary conditions) demonstrate reasonable agreement with experimental data.

Since the energy spectrum of 2D electrons in nonsymmetric heterostructures is spin-split, then spin-flip transitions appear the dominant contribution to the PD current excited by far-infrared radiation. To the best of our knowledge the contribution from the spin-flip transitions to the PD current was only previously considered for bulk *p*-type Ge,[17] where mid-IR excitation is effective. The scheme of intersubband transitions between spin-split electron states is presented in Fig. 1(a) where the spin-split energy is determined as $2v_s p_F$, where p_F denotes the Fermi moment and v_s is the characteristic spin velocity. The geometry of THz excitation is shown in Fig. 1(b). Due to the presence of two distinct directions in the 2D plane (i.e., the longitudinal wave vector $\mathbf{q}$ direction and the perpendicular direction $[\mathbf{q}\times\mathbf{v}_s]$; the vec-

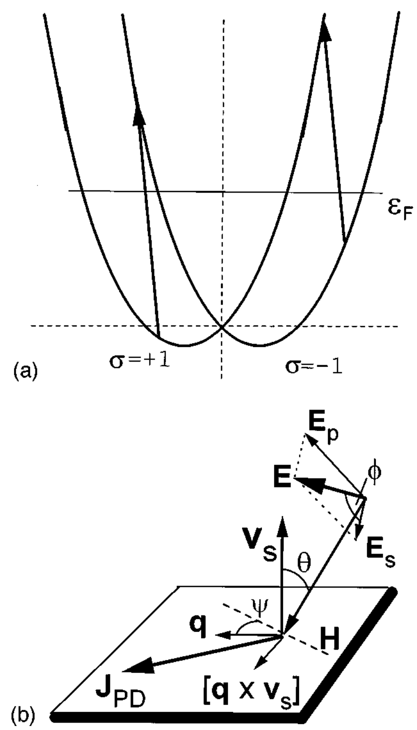

FIG. 1. The scheme of the nonvertical spin-flip transitions (a) and the geometry for excitation of the longitudinal and transverse PD-currents (b). Here $\sigma=\pm1$ are the quantum numbers for the spin-split branches of the energy spectra, $\mathbf{q}$ is the longitudinal component of the wave vector, $\mathbf{H}$ is the magnetic field, $\mathbf{v}_s$ is the characteristic spin velocity, and the angles θ, ϕ, and ψ characterize the geometry.

tor $\mathbf{v}_s$ is along the normal to 2D plane) the matrix elements for spin-flip transitions shows a complicated angular form and the PD current is not parallel to the transferred momentum $\hbar\mathbf{q}$. The calculations of these dependencies of the PD current, which also take into account the effect of an in-plane magnetic field, are presented below (previously we considered this problem in the absence of magnetic field[18]).

Due to the effect of the in-plane magnetic field [vector $\mathbf{H}$ in Fig. 1(b)], the branches of the energy spectra belonging to different spin states are shifted in the $\mathbf{p}$ plane along the direction perpendicular to $\mathbf{H}$. The electron energy spectrum for such a case appears to break the inversion symmetry along this direction (such peculiarity of the spectra and its effect on the transport phenomena are discussed in Refs. 19–21) and, therefore, both the conservation laws for energy and momenta transfer under intersubband transitions and the corresponding matrix elements are modified in an essential manner. This leads to substantial modifications of the spectral and angular dependencies of the PD current under relatively weak magnetic fields when the Pauli spin-split energy is comparable with the energy of the intersubband transition, $2v_s p_F$.

The kinetic approach for the calculations of PD currents in 2D systems under resonant intersubband excitation was worked out in Refs. 22 and 23 (see also Ref. 24 where the transitions between Landau subbands in bulk conductors were considered). The photoresponse was deduced from the quantum kinetic equation averaged over the period of excitation. The matrix elements of the intersubband transitions that appear in the generation rate of such a kinetic equation take exactly into account the momentum transfer. As a mechanism of momentum relaxation we consider below the scattering by static defects (this mechanism is particularly relevant in the low-temperature region) and the intersubband transition broadening is described by the phenomenological energy parameter Γ. The second-order responses have been calculated for the quasiequilibrium Fermi distribution of electrons using an effective electron temperature.

Below, after presenting the details of our calculations for the PD current density (Sec. II), we consider the spectral and angular dependencies of the PD current, and then discuss the effect of the in-plane magnetic field (Secs. III A and III B, respectively). In the final section conclusions and the list of assumptions are presented. Some details about the determination of the energy spectrum and matrix element for the spin-flip transitions are given in Appendix A, while Appendix B contains the estimation of the small quantum correction to the PD current.

II. THEORETICAL BACKGROUND

The Hamiltonian for the lower spin-split subband in nonsymmetric heterostructures is given by the 2×2 matrix[8,9]

$$\hat{h}=\frac{p^2}{2m}+(\hat{\boldsymbol{\sigma}}\cdot\mathbf{w}_{\mathbf{p}}),\quad \mathbf{w}_{\mathbf{p}}=[\mathbf{v}_s\times\mathbf{p}]+\frac{g}{2}\mu_B\mathbf{H}. \tag{1}$$

Here $\mathbf{p}$ is the 2D momentum, m is the effective mass, $\hat{\boldsymbol{\sigma}}$ is the Pauli matrices; the g factor and Bohr magneton g and μ_B are determined by the spin-splitting energy for $\mathbf{p}=0$ under the in-plane magnetic field $\mathbf{H}$ [we neglected here the usual magnetoinduced modification of the kinetic energy in Eq. (1) using the condition $eHd/c\ll p_F$; d is the QW width]. The spin velocity $\mathbf{v}_s$ is determined by the nonsymmetric confined potential, and such velocity is used below as a given band-structure parameter. The spin-dependent dispersion law $\varepsilon_{\sigma\mathbf{p}}$ is obtained from the eigenstate problem $\hat{h}|\sigma\mathbf{p}\rangle=\varepsilon_{\sigma\mathbf{p}}|\sigma\mathbf{p}\rangle$. The results for $\varepsilon_{\sigma\mathbf{p}}$ and for wave functions $|\sigma\mathbf{p}\rangle$ are evaluated after diagonalization of Hamiltonian (1). See Appendix A for the details. The dispersion law appears to depend on the spin quantum numbers $\sigma=\pm 1$ in the following way: $\varepsilon_{\sigma\mathbf{p}}=p^2/(2m)+\sigma w_{\mathbf{p}}$; note the nonsymmetry of this energy spectrum ($\varepsilon_{\sigma-\mathbf{p}}\neq\varepsilon_{\sigma\mathbf{p}}$) in the presence of the in-plane magnetic field. The corresponding wave functions take forms:

$$|\sigma\mathbf{p}\rangle=\frac{1}{\sqrt{2}}\left[1+i\frac{\hat{\boldsymbol{\sigma}}\cdot[\mathbf{w}_{\mathbf{p}}\times\mathbf{v}_s]}{w_{\mathbf{p}}v_s}\right]|\sigma\rangle,\quad \hat{\sigma}_z|\sigma=\sigma|\sigma\rangle, \tag{2}$$

where $|\sigma\rangle$ are the two-component columns with the projections ± 1 on the OZ axis.

The general expression for the photon-induced steady-state current density $\mathbf{J}_{PD}$ normalized to the area L^2 is written by the usual way:

$$\mathbf{J}_{PD}=\frac{e}{L^2}sp\left(\frac{\mathbf{p}}{m}+[\hat{\boldsymbol{\sigma}}\times\mathbf{v}_s]\right)\overline{\hat{\rho}}+\delta\mathbf{J}, \tag{3}$$

where sp is included in the summations over $\mathbf{p}$ and the spin variable, $\overline{\hat{\rho}}$ is averaged over the period of the radiation density matrix, and spin-dependent contributions to the velocity operator $[\hat{\boldsymbol{\sigma}}\times\mathbf{v}_s]$ are taken into account. The small quantum correction $\delta\mathbf{J}$ is considered in Appendix B. The averaged density matrix $\overline{\hat{\rho}}$ may be found from the quantum-kinetic equation:

$$\frac{i}{\hbar}[\hat{h},\overline{\hat{\rho}}]_-=\hat{J}_{sc}(\overline{\hat{\rho}})+\hat{G}(\overline{\hat{\rho}}),$$

$$\hat{G}=\frac{1}{\hbar^2}\int_{-\infty}^{0}d\tau e^{-i(\omega+i\lambda)\tau}\times[e^{(i/\hbar)\hat{h}\tau}[\delta\hat{h},\overline{\hat{\rho}}]e^{-(i/\hbar)\hat{h}\tau},\delta\hat{h}^+]_-+\text{h.c.} \tag{4}$$

Here, $\hat{J}_{sc}$ is the usual collision integral and $\hat{G}$ describes the photon-induced transition generation rate through the operator $\widehat{\delta h}$ given by:

$$\widehat{\delta h}=-i\frac{e/\omega}{2m}\mathbf{E}\cdot(\hat{\mathbf{p}}e^{i\mathbf{qx}}+e^{i\mathbf{qx}}\hat{\mathbf{p}})+i\frac{e}{\omega}\hat{\boldsymbol{\sigma}}\cdot[\mathbf{v}_s\times\mathbf{E}]e^{i\mathbf{qx}}+\frac{g\mu_B}{2}\frac{c}{\omega}(\hat{\boldsymbol{\sigma}}\cdot[\mathbf{q}\times\mathbf{E}])e^{i\mathbf{qx}}. \tag{5}$$

This perturbation operator originates in the general Hamiltonian, linearized in the pumping wave $\mathbf{E}\exp(i\mathbf{qx}-i\omega t)$. Note that $\mathbf{q}$ is the longitudinal component of the photon wave vector (ω and $\mathbf{E}$ are the frequency of wave and the electric-field strength) while the transversal component is omitted here because the width of the 2D layer is smaller than photon wavelength.

In this paper we consider the case where the effect of spin splitting is not suppressed by scattering ($\overline{\tau}$ is the characteristic relaxation time), i.e.,

$$2v_s p_F \gg \hbar/\overline{\tau}, \tag{6}$$

and the nondiagonal component of $\hat{\rho}$ is small so that the spin-flip contribution to velocity operator in Eq. (3) may be neglected. The diagonal component of the kinetic equation needs for this case only: $G(f|\alpha)+J_{sc}(f|\alpha)=0;\ \alpha=(\sigma,\mathbf{p})$. The generation rate transforms as

$$G(f|\alpha)=\frac{2\pi}{\hbar}\sum_{\alpha'}\ [|(\alpha|\delta\hat{h}|\alpha')|^2\delta_\Gamma(\varepsilon_\alpha-\varepsilon_{\alpha'}-\hbar\omega)$$
$$+|(\alpha|\delta\hat{h}^+|\alpha')|^2\delta_\Gamma(\varepsilon_\alpha-\varepsilon_{\alpha'}+\hbar\omega)](f_\alpha-f_{\alpha'}), \tag{7}$$

while the collision integral takes the usual form for the elastic scattering case:

$$J_{sc}(f|\alpha)=\sum_{\alpha'}\ W(\alpha,\alpha')(f_{\alpha'}-f_\alpha),$$

$$W(\alpha,\alpha')=\frac{2\pi}{\hbar}\sum_{\mathbf{k}}\ w_k|\langle\alpha|e^{i\mathbf{kx}}|\alpha'\rangle|^2\delta(\varepsilon_\alpha-\varepsilon_{\alpha'}). \tag{8}$$

The probability of transitions in Eq. (8), $W(\alpha,\alpha')$, is written for the static random potential scattering case (w_k is correlation function of random potentials and $\hbar\mathbf{k}$ is transferred electron momentum).

Since the anisotropic part of $G(f|\sigma\mathbf{p})$ is small (due to the smallness of the transferred momentum) we can consider the linearized kinetic equation

$$J_{sc}(\delta f|\sigma\mathbf{p})+\delta G^{(eq)}_{\sigma\mathbf{p}}=0, \tag{9}$$

where $\delta f_{\sigma\mathbf{p}}$ is the anisotropic part of the electron distribution function. The generation rate $\delta G^{(eq)}_{\sigma\mathbf{p}}$, linear in $\hbar\mathbf{q}$, is calculated by using the equilibrium electron distribution in Eq. (7). For simplicity we consider below short-range scattering for which the solution of Eq. (9) may be written as

$$\delta f_{\sigma\mathbf{p}}=\tau_{\sigma\mathbf{p}}\delta G^{(eq)}_{\sigma\mathbf{p}},\quad (\tau_{\sigma\mathbf{p}})^{-1}=\overline{w}\frac{2\pi}{\hbar}\sum_{\mathbf{p}'}\ \delta(\varepsilon_{\sigma\mathbf{p}}-\varepsilon_{\sigma\mathbf{p}'}), \tag{10}$$

and the relaxation time $\tau_{\sigma\mathbf{p}}$ is expressed through the 2D density of states ($\overline{w}$ is the short-range correlator of scattering potentials).

The PD current density is obtained after substitution (10) into Eq. (3). For heavy-doped structures [with $\varepsilon_F=p_F^2/(2m)$] we can use the inequalities

$$\varepsilon_F \gg mv_s^2/2,\quad g\mu_B H, \tag{11}$$

and take into account contributions to the matrix elements of the intersubband transitions [Eq. (A11)], which are linear with respect to $\hbar\mathbf{q}$. It should be noted that the Pauli-type spin-flip interaction [last term in Eq. (5)] drops out of the calculations in the first order with respect to $\hbar\mathbf{q}$ because this contribution to Eq. (A8) is proportional to $\delta_{\mathbf{pp}'}$ and describes vertical transitions only. The total PD current contains two contributions $\mathbf{j}^{(1)}$ and $\mathbf{j}^{(2)}$ resulting from the expansion of the matrix elements and the energy conservation law, respectively. For the quasiequilibrium Fermi distribution $f_T(\varepsilon_{\sigma\mathbf{p}})$ with the electron temperature T we write the first contribution using Eq. (A11) as follows:

$$\mathbf{j}^{(1)}\simeq-\frac{e^3\overline{\tau}}{m\omega}\int\frac{d\mathbf{p}}{2\pi\hbar^2}\mathbf{p}\left(\frac{v_s}{w^{\mathbf{p}}}\right)^2(\mathbf{E}\cdot\mathbf{w}_\mathbf{p})(\mathbf{E}\cdot[\mathbf{v}_s\times\hbar\mathbf{q}])$$
$$\times\delta_\Gamma(\varepsilon_{+1\mathbf{p}}-\varepsilon_{-1\mathbf{p}}-\hbar\omega)\{f_T'(\varepsilon_{+1\mathbf{p}})+f_T'(\varepsilon_{-1\mathbf{p}})\}. \tag{12}$$

The second contribution is included [Eq. (A10)] and transforms as

$$\mathbf{j}^{(2)}\simeq\frac{e^3\overline{\tau}}{m\omega}\int\frac{d\mathbf{p}}{2\pi\hbar^2}\mathbf{p}\frac{(\mathbf{p}\cdot\hbar\mathbf{q})}{m}\left(\frac{v_s}{w_\mathbf{p}}\right)^2(\mathbf{E}\cdot\mathbf{w}_\mathbf{p})^2$$
$$\times\delta_\Gamma'(\varepsilon_{+1\mathbf{p}}-\varepsilon_{-1\mathbf{p}}-\hbar\omega)\{f_T'(\varepsilon_{+1\mathbf{p}})-f_T'(\varepsilon_{-1\mathbf{p}})\}. \tag{13}$$

Here [and in Eq. (7)] we took into account the broadening of the spin-flip intersubband transitions using $\delta_\Gamma(E)=\Gamma/[\pi(E^2+\Gamma^2)]$, when Γ is the broadening energy. The inequalities (11) give us $|\mathbf{w}_\mathbf{p}|\ll\varepsilon_F$, and for such approximation $\mathbf{j}^{(1,2)}$ are transformed to

$$\mathbf{j}^{(1)}\simeq-\frac{e^3\overline{\tau}}{m\omega}\int\frac{d\mathbf{p}}{\pi\hbar^2}\mathbf{p}\left(\frac{v_s}{w_\mathbf{p}}\right)^2$$
$$\times(\mathbf{E}\cdot\mathbf{w}_\mathbf{p})(\mathbf{E}\cdot[\mathbf{v}_s\times\hbar\mathbf{q}])\delta_\Gamma(2|\mathbf{w}_\mathbf{p}|-\hbar\omega)f_T(\varepsilon_p),$$

$$\mathbf{j}^{(2)}\simeq\frac{e^3\overline{\tau}}{m\omega}\int\frac{d\mathbf{p}}{\pi\hbar^2}\mathbf{p}\frac{(\mathbf{p}\cdot\hbar\mathbf{q})}{m}\frac{v_s^2}{w_\mathbf{p}}$$
$$\times(\mathbf{E}\cdot\mathbf{w}_\mathbf{p})^2\delta_\Gamma'(2|\mathbf{w}_\mathbf{p}|-\hbar\omega)f_T'(\varepsilon_p), \tag{14}$$

where $\varepsilon_p=p^2/2m$ is the electron dispersion law for the spin-degenerate case. Due to complicated angular dependencies of the matrix elements (A11) the PD currents $\mathbf{j}^{(1,2)}$ are not parallel to $\hbar\mathbf{q}$ and a *transverse* (i.e., parallel to $[\hbar\mathbf{q}\times\mathbf{v}_s]$) component of the PD current appears in Eq. (14).

III. SPECTRAL AND ANGLE DEPENDENCIES

Thus, the dependencies of the PD current density $\mathbf{j}^{(1)}+\mathbf{j}^{(2)}$ on the frequency and angles [incidence and polarization angles θ and ϕ in Fig. 1(b), and ψ, the angle between the magnetic field $\mathbf{H}$ and the in-plane wave vector $\mathbf{q}$] are determined after integration of Eq. (14) over the $\mathbf{p}$ plane. Below we consider first the zero magnetic-field case and then we discuss the effect of an in-plane magnetic field.

A. Zero magnetic-field case

In this case $\mathbf{w}_\mathbf{p}=[\mathbf{v}_s\times\mathbf{p}]$ and integration over the $\mathbf{p}$ plane angle φ yields the following contributions to $\mathbf{j}^{(1,2)}$:

$$\int_0^{2\pi}\frac{d\varphi}{2\pi}\mathbf{p}(\mathbf{E}\cdot[\mathbf{v}_s\times\mathbf{p}])=\frac{p^2}{2}[\mathbf{E}\times\mathbf{v}_s],$$

$$\int_0^{2\pi}\frac{d\varphi}{2\pi}\mathbf{p}(\hbar\mathbf{q}\cdot\mathbf{p})(\mathbf{E}\cdot[\mathbf{v}_s\times\mathbf{p}])^2 \tag{15}$$

$$=\frac{p^4}{8}\{\hbar\mathbf{q}[\mathbf{E}\times\mathbf{v}_s]^2+2[\mathbf{E}\times\mathbf{v}_s](\hbar\mathbf{q}\cdot[\mathbf{E}\times\mathbf{v}_s])\}.$$

The integrations over $|\mathbf{p}|$ are straightforward for the zero-temperature case due to the replacement of f_T and f_T' by the δ and δ' functions, respectively, and then we have obtained the explicit expressions for PD current density. It is convenient to introduce the PD velocity $\mathbf{V}_{PD}$ according to

$$en_{2D}\mathbf{V}_{PD}=\mathbf{j}^{(1)}+\mathbf{j}^{(2)}, \tag{16}$$

$$\mathbf{V}_{PD}=V_{PD}^{\parallel}\frac{\mathbf{q}}{q}+V_{PD}^{\perp}\frac{[\mathbf{q}\times\mathbf{v}_s]}{qv_s},$$

where we used $\mathbf{q}$ and $[\mathbf{q}\times\mathbf{v}_s]$ as the basic directions in the 2D plane; $V_{PD}^{\parallel}$ and $V_{PD}^{\perp}$ are the longitudinal and transverse components of the PD velocity.

The explicit expressions for $V_{PD}^{\parallel,\perp}$ take the forms

$$\left|\begin{matrix}V_{PD}^{\parallel}\\ V_{PD}^{\perp}\end{matrix}\right|=-\pi\frac{e^2\overline{\tau}}{m\omega}\frac{v_s^2}{\varepsilon_F}\hbar q\left\{\left|\begin{matrix}E_s^2\\ E_sE_p\cos\theta\end{matrix}\right|\delta_\Gamma(2v_sp_F-\hbar\omega)\right.$$
$$\left.-2v_sp_F\left|\begin{matrix}3E_s^2+E_p^2\cos^2\theta\\ 2E_sE_p\cos\theta\end{matrix}\right|\left[v_sp_F\delta_\Gamma''(2v_sp_F-\hbar\omega)+\frac{3}{2}\delta_\Gamma'(2v_sp_F-\hbar\omega)\right]\right\}. \tag{17}$$

It is convenient to express $V_{PD}^{\parallel,\perp}$ through the angle-dependent functions

$$\Phi_{\parallel}(\theta,\phi)=(3\cos^2\phi+\sin^2\phi\cos^2\theta)\sin\theta,$$

$$\Phi_{\perp}(\theta,\phi)=(\sin 2\theta\sin 2\phi)/2 \tag{18}$$

and the dimensionless frequency detuning

$$\Omega=(\hbar\omega-2v_sp_F)/\Gamma, \tag{19}$$

so that spectral dependencies are written in terms of $\Delta(\Omega)=(\Omega^2+1)^{-1}$ and the first and second derivatives of this function $\Delta'(\Omega)$ and $\Delta''(\Omega)$. As a result we obtain

$$V_{PD}^{\parallel}=-v_{PD}\{[f\Delta''(\Omega)+\Delta'(\Omega)]\Phi_{\parallel}(\theta,\phi)$$
$$+(8/9f)\Delta(\Omega)\cos^2\phi\sin\theta\},$$
$$V_{PD}^{\perp}=-v_{PD}[f\Delta''(\Omega)+\Delta'(\Omega) \tag{20}$$
$$+(4/9f)\Delta(\Omega)]\Phi_{\perp}(\theta,\phi),$$

where the dimensionless parameter $f=2v_sp_F/(3\Gamma)$ describes the broadening effect and this parameter is usually larger than unity due to the inequality (6). We have also introduced the characteristic velocity, v_{PD}, according to

$$v_{PD}=\frac{v_s^3}{cv_F}\frac{S}{S_{PD}},\quad S_{PD}^{-1}=12\pi\frac{e^2}{\hbar c}\frac{\overline{\tau}}{m}\left(\frac{\hbar}{\Gamma}\right)^2, \tag{21}$$

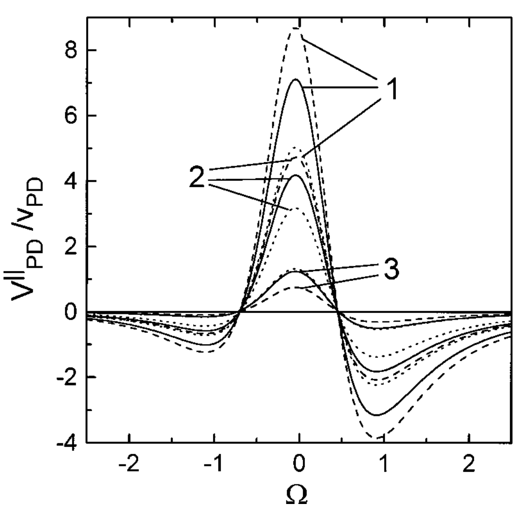

FIG. 2. Spectral dependencies of the longitudinal components of the PD current under, respectively, s polarized (1), mixed (2, with $\phi=\pi/4$,) and p polarized (3) THz pump excitation for the incident angles: $\theta=\pi/6$ (dashed lines), $\theta=\pi/4$, (solid lines), and $\theta=\pi/3$ (dotted lines).

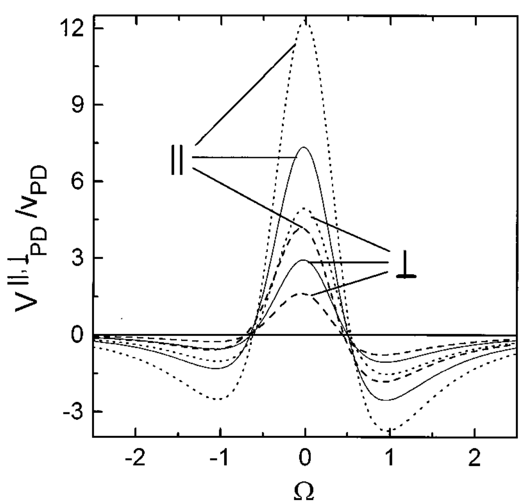

FIG. 3. Spectral dependencies for the longitudinal (∥) and transverse (⊥) components of the PD current for the angles $\theta=\phi=\pi/4$ and the different broadening parameters, namely, $f=1.74$ (dashed lines), $f=3$ (solid lines), and $f=5$ (dotted lines).

where S is the magnitude of the Poynting vector of the THz pump and S_{PD} is the characteristic intensity; v_F is the Fermi velocity.

Below, numerical estimations are presented for a InAs-based quantum well with electron concentration $1.2\times 10^{12}\ \mathrm{cm}^{-2}$ and mobility $9.6\times 10^4\ \mathrm{cm}^2$ V/s (the parameters are taken from Ref. 12). In accordance with experimental data in Refs. 12 and 13 we choose $v_s \simeq 7.2\times 10^5$ cm/s so that the energy of the transition $2v_s p_F \simeq 3.5$ meV corresponds to the 0.75 THz excitation. Assuming $\Gamma \simeq \hbar/\overline{\tau}$ we obtain from Eq. (21) a characteristic velocity v_{PD} around 25 cm/s for a pump intensity of the order of 1 kW/cm^2, and $\Omega \simeq 0$. The estimation of the dimensionless broadening is $f \simeq 1.8$ for such a set of parameters. Maximum values of $V_{PD}^{\parallel,\perp}$ are a few times larger than v_{PD} due to the spectral dependent factors in Eq. (20) (the peak values of $V_{PD}^{\parallel,\perp}$ are up to 200 cm/s for the conditions under consideration). The resonant spectral dependencies of $V_{PD}^{\parallel,\perp}$ described by Eq. (20) show *double* spectral inversion character and the spectra are essentially changed under variations of the angles of the incidence or polarization. In Fig. 2 we have plotted these dependencies for the longitudinal component of PD velocity. The angle dependencies of $V_{PD}^{\perp}$ are completely determined by $\Phi_{\perp}(\theta,\phi)$. The maximum value of $V_{PD}^{\perp}$ is realized for $\phi = \pi/4$ while the transverse component of the PD current does not excite by pure *s*- or *p*-polarized pumps. The spectral dependencies of $V_{PD}^{\perp}$ also show a double spectral inversion as one may see from Fig. 3. From this figure, one furthermore sees that the $V_{PD}^{\parallel,\perp}$ peaks grow when the broadening parameter f increases (i.e., collisions become less important).

B. Effect of the in-plane magnetic field

Due to the effect of the magnetic field, $|\mathbf{w_p}|$ depends on the angle φ and the averaging in Eq. (15) is no longer possible. For such a case the explicit expressions for $V_{PD}^{\parallel,\perp}$ can be obtained after transformation of Eq. (14) to the form:

$$\left|\begin{matrix} V_{PD}^{\parallel} \\ V_{PD}^{\perp}\end{matrix}\right| \simeq \frac{e^2\overline{\tau}}{m\omega}\frac{v_s^2}{n_{2D}}\int \frac{d\mathbf{p}}{\pi\hbar^2}\left|\begin{matrix} (\hbar\mathbf{q}\cdot\mathbf{p})/(\hbar q) \\ (\mathbf{p}\cdot[\hbar\mathbf{q}\times\mathbf{v}_s])/(\hbar q v_s)\end{matrix}\right| \left\{ \frac{(\mathbf{E}\cdot\mathbf{w_p})}{w_{\mathbf{p}}^2}(\mathbf{E}\cdot[\mathbf{v}_s\times\hbar\mathbf{q}])\,\delta_\Gamma(2|\mathbf{w_p}|-\hbar\omega)f_T(\varepsilon_p) + \frac{(\hbar\mathbf{q}\cdot\mathbf{p})}{m w_{\mathbf{p}}}(\mathbf{E}\cdot\mathbf{w_p})^2\,\delta'_\Gamma(2|\mathbf{w_p}|-\hbar\omega)f'_T(\varepsilon_p)\right\}. \tag{22}$$

The integration over φ cannot be performed analytically here, and after integration over $|\mathbf{p}|$ (for the zero-temperature case), Eq. (22) is rewritten as

$$\left|\begin{matrix} V_{PD}^{\parallel} \\ V_{PD}^{\perp}\end{matrix}\right| \simeq -v_{PD}\sin\theta\frac{8}{3\pi}\int_0^{2\pi}d\varphi\frac{\mathcal{A}_{\varphi w}}{v_\varphi}\left|\begin{matrix}\sin(\varphi+\psi) \\ -\cos(\varphi+\psi)\end{matrix}\right|\left\{\frac{3f}{2}\Delta''(\Omega_\varphi)\mathcal{A}_{\varphi w}\sin(\varphi+\psi)\frac{1+w\cos\varphi}{v_\varphi} + \Delta'(\Omega_\varphi)\sin(\varphi+\psi)\left[\mathcal{A}_{w\varphi}\left(1-\frac{1+w\cos\varphi}{2v_\varphi^2}\right)+\mathcal{A}_{\varphi w=0}\right] + \Delta(\Omega_\varphi)\frac{\cos\phi}{3f}\frac{1+w\cos\varphi}{v_\varphi}\right\}. \tag{23}$$

Here we have introduced the angle-dependent functions:

$$\mathcal{A}_{\varphi w} = w(\cos\phi\sin\psi + \sin\phi\cos\theta\cos\psi) + \cos\phi\sin(\varphi+\psi) - \sin\phi\cos\theta\cos(\varphi+\psi),$$
$$v_\varphi = \sqrt{1+w^2+2w\cos\varphi}, \quad \Omega_\varphi = \Omega + 3f(v_\varphi - 1), \tag{24}$$

when $w = g\mu_B H/(2v_s p_F)$ is a dimensionless quantity characterizing the effect of the magnetic field. The integral (23) is not convergent at $\varphi=\pi$ for $w=1$ due to divergence of the matrix element (A11) when the cross point of the energy branches (the point of the **p**-plane with $|\mathbf{w_p}|=0$) intersects by the Fermi level. Both finite-temperature effects [which are described by Eq. (22)] and scattering by magnetic impurities (the presence of which breaks the degeneracy of the energy spectra) are essential at $w=1$.

Based on Eq. (23) results of numerical calculations of PD velocities, $V_{PD}^{\parallel,\perp}$ are presented below using the parameters listed in Sec. III A. Since the dependencies $V_{PD}^{\parallel,\perp}$ vs w are under consideration below (w is of the order of unit if the magnetic field is around 1 T) we do not need any concrete value of the g factor.[25] The modifications of the spectral dependencies with increasing magnetic field are shown in Figs. 4 and 5. For the case of the strong magnetic field ($w \gg 1$) we use $v_\varphi \simeq w$, $\mathcal{A}_{\varphi w} \simeq w\cos(\mathbf{E},\mathbf{H})$ and Eq. (23) is estimated bythe simple Eqs.

$$V_{PD}^{\parallel}/v_{PD} \simeq -\frac{8}{3}w\Delta'(\Omega_H)\sin\theta\cos^2(\mathbf{E},\mathbf{H}) + o(\mathrm{const}),$$
$$V_{PD}^{\perp}/v_{PD} \simeq o(\mathrm{const}), \quad \Omega_H = (\hbar\omega - g\mu_B H)/\Gamma. \tag{25}$$

The longitudinal component of the PD velocity increases proportionally to w, and the δ'-like peculiarity shifts to

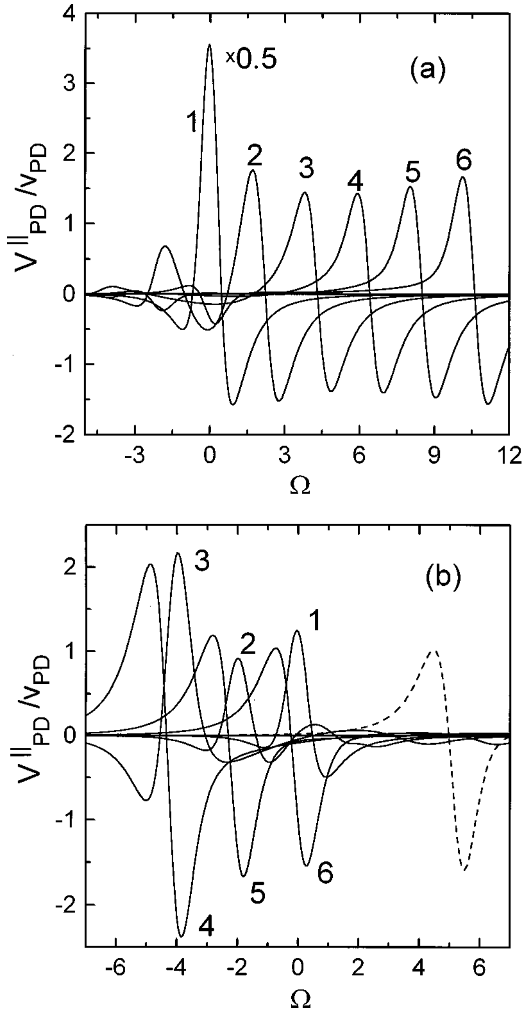

FIG. 4. Spectral dependencies of the longitudinal component of the PD current under *s* polarized (a) and *p* polarized (b) THz pump excitation for different magnetic fields, viz., $w=0$ (1), $w=0.4$ (2), $w=0.8$ (3), $w=1.2$ (4), $w=1.6$ (5), and $w=2$ (6) (the dashed curve in (b) corresponds to $w=3$). The incidence angle and the orientation of the magnetic field are $\theta=\pi/4$ and $\psi=\pi/4$, respectively.

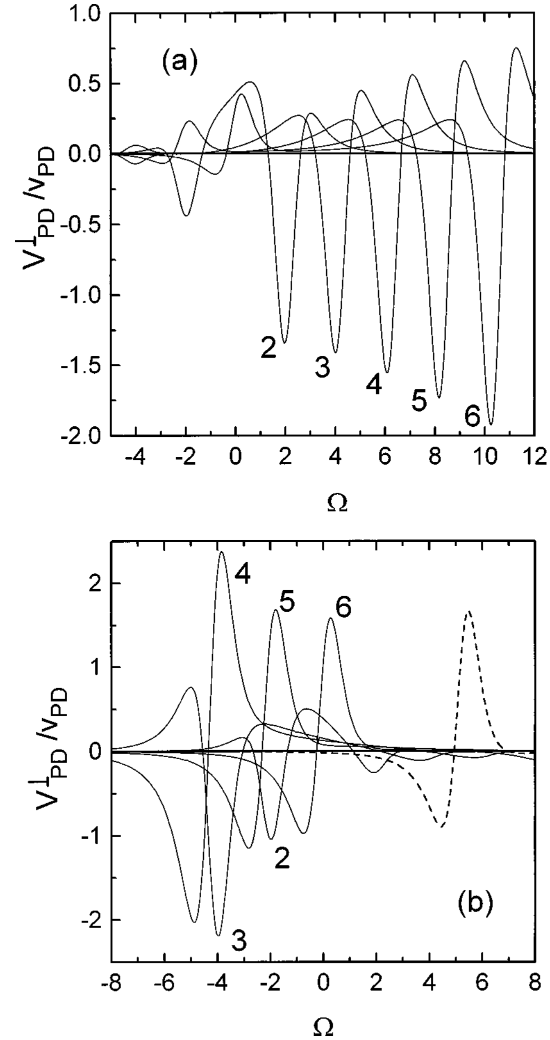

FIG. 5. The same as in Figs. 4(a) and 4(b) for the transverse component of the PD current.

strong magnetic fields while the transverse component of the PD velocity still stay proportional to a constant. These transformations of $V^{\parallel}_{PD}$ for intermediate values of *w* are shown in Fig. 4(a) for the *s*-polarized pump. Analogous transformations take place for the transverse component of the PD velocity under the *s*-polarized pump [see Fig. 5(a)] but $V^{\perp}_{PD}=0$ if $w=0$ for this geometry; an in-plane magnetic field invalidates this selection rule. The modifications of the spectra in the case of a *p*-polarized pump are found to be more complicated for intermediate *w*'s [see Figs. 4(b) and 5(b)], i.e., peaks shift to lower Ω if $w<1$ and transformation to the strong magnetic field case begins for $w>1$. Significant modifications of $V^{\parallel,\perp}_{PD}$ under variation of the magnetic field orientation are shown in Figs. 6(a) and 6(b) (due to symmetry requirements $V^{\parallel,\perp}_{PD}$ does not change under the replacements $\mathbf{H}\to-\mathbf{H}$ and $\mathbf{E}_s\to-\mathbf{E}_s$ so that we consider the region $0<\psi<\pi/2$ only). Note also that the transverse component of the PD velocity vanishes for $\psi=0$, $\psi=\pi/2$, and the spectral dependencies under consideration exhibit a complicated oscillatory behavior.

IV. CONCLUSION

In this paper we have demonstrated that the photon drag current caused by nonvertical spin-flip transitions of 2D electrons in nonsymmetric QW's is detectable and exhibits complicated geometrical dependencies of the angles of incidence and polarization and on the in-plane orientation of the magnetic field. The mechanism under consideration is characterized by the occurrence of a transverse component of the current and a double spectral inversion of the photoresponse. The mechanism is sensitive even to the moderate in-plane magnetic field. The above-mentioned features allows one to separate the spin-flip PD current from those originating in other types of transitions. The effective photoresponse under consideration may lead to possibilities to develop a type of ultrafast detector for the THz spectral region.

The presented results were calculated under the following assumptions. The model of electron states introduced by Eq. (1) is based on the simple effective mass approximation and does not take into account both self-consistent corrections and the effect of nonparabolicity. These effects do not change the structure of the Hamiltonian (1) and they are taken into account if we consider *m*, *g*, and v_s as semiphenomenological parameters. The assumption of short-range

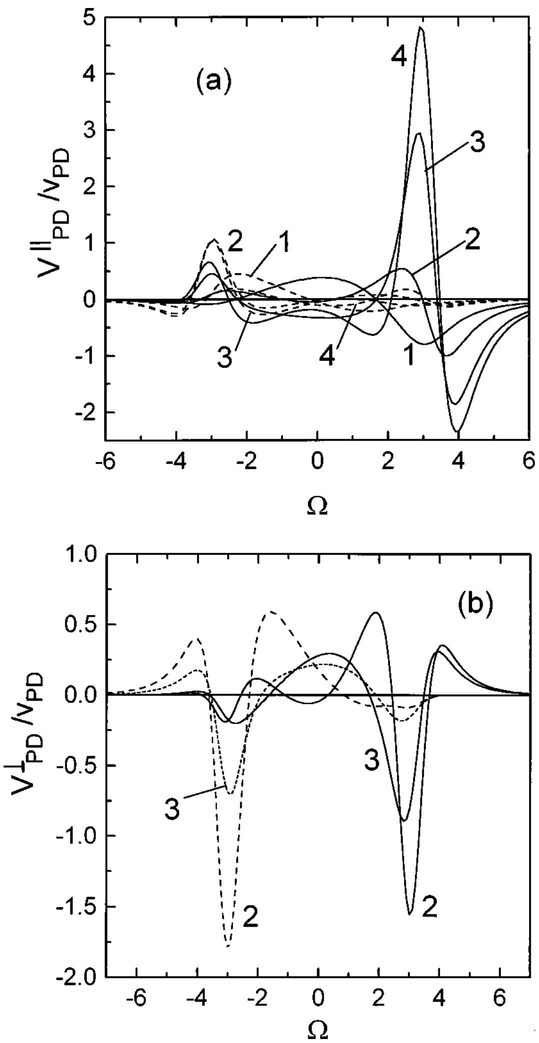

FIG. 6. Spectral dependencies for the longitudinal (a) and transverse (b) components of the PD current under *s* polarized (solid curves) and *p* polarized (dashed curves) THz pump excitation for $\theta=\pi/4$ and the following orientations of the magnetic field: $\psi=0$ (1), $\psi=\pi/6$ (2), $\psi=\pi/3$ (3), and $\psi=\pi/2$ (4). The dimensionless magnetic field is $w=0.6$.

scattering has been used above for the sake of simplicity only (one can consider $\overline{\tau}$ as a momentum relaxation time at the Fermi energy). The phenomenological description of the broadening of the spin-flip transitions is generally accepted and such approach gives realistic shapes of absorption peak [we suppose that Γ is bigger than the temperature in order to perform the integration of Eq. (14), and this condition is usually valid for the low temperature region]. The inequality (6) is satisfied for samples with high mobility.[12,13] Because the calculations of the generation rate in Eq. (9), based on the use of the equilibrium electron distribution, are valid for the description of the second-order photoresponse, then the effect of electron heating is not essential. Our numerical results confines this expectation. The local-field corrections change the shape of the peaks but do not affect the angle of incidence and polarization dependencies; these modifications of the spectra can be taken into account through a change of the phenomenological parameters introduced above. For a closer examination of the response at $w=1$ both the temperature-dependence of the Fermi distribution and the scattering by magnetic impurities must be taken into account. We did not consider this case because peculiarities of the PD current appears in a narrow region of w around $w=1$ and more sensitive magnetotransport measurements seems needed to study this case. One should note also that photogalvanic contributions to the photoresponse can appear under in-plane magnetic fields;[21] such type of response does not depend on $\mathbf{q}$ and may be separated if one changes the geometry of excitation in such a way that $\mathbf{q}\rightarrow-\mathbf{q}$. All assumptions discussed above do not change significantly the value of the PD current and the described spectral/angular dependencies. More detailed numerical calculations are needed for concrete cases.

In a broader perspective it appears that the spin-flip transitions of 2D electrons in narrow-gap nonsymmetric heterostructures contribute essentially to the photoresponse under THz excitation. This might stimulate experimental examinations of both PD currents and other types of responses (photoconductivity, photoinduced voltage) in InAs-based heterostructures.

APPENDIX A

Expressions for the energy spectrum and wave functions (2) are evaluated below through a diagonalization of the Hamiltonian in Eq. (1), which is performed by the unitary transformation

$$\hat{U}_{\mathbf{p}}=\frac{1+i\hat{\boldsymbol{\sigma}}\cdot\mathbf{u}_{\mathbf{p}}}{\sqrt{2}}, \tag{A1}$$

where the condition $(\hat{U}_{\mathbf{p}}^{+}\hat{U}_{\mathbf{p}})=1$ is satisfied if $(\mathbf{u}_{\mathbf{p}}\cdot\mathbf{u}_{\mathbf{p}})=1$. In order to fix the orientation of the unit vector $\mathbf{u}_{\mathbf{p}}$ introduced in Eq. (A1), we consider the matrix contribution to the Hamiltonian

$$\hat{U}_{\mathbf{p}}^{+}(\hat{\boldsymbol{\sigma}}\cdot\mathbf{w}_{\mathbf{p}})\hat{U}_{\mathbf{p}}=\frac{1}{2}\{(\hat{\boldsymbol{\sigma}}\cdot\mathbf{w}_{\mathbf{p}})+(\hat{\boldsymbol{\sigma}}\cdot\mathbf{u}_{\mathbf{p}})(\hat{\boldsymbol{\sigma}}\cdot\mathbf{w}_{\mathbf{p}})(\hat{\boldsymbol{\sigma}}\cdot\mathbf{u}_{\mathbf{p}}) + i[(\hat{\boldsymbol{\sigma}}\cdot\mathbf{w}_{\mathbf{p}}),(\hat{\boldsymbol{\sigma}}\cdot\mathbf{u}_{\mathbf{p}})]_{-}\}, \tag{A2}$$

and note that under the condition $\mathbf{w}_{\mathbf{p}}\perp\mathbf{u}_{\mathbf{p}}$, Eq. (A2) may be transformed into diagonal form, i.e.,

$$\hat{U}_{\mathbf{p}}^{+}(\hat{\boldsymbol{\sigma}}\cdot\mathbf{w}_{\mathbf{p}})\hat{U}_{\mathbf{p}}=(\hat{\boldsymbol{\sigma}}\cdot[\mathbf{u}_{\mathbf{p}}\times\mathbf{w}_{\mathbf{p}}])=\hat{\sigma}_{z}w_{\mathbf{p}}. \tag{A3}$$

As a result the diagonalized Hamiltonian takes the form

$$\hat{U}_{\mathbf{p}}^{+}\hat{h}\hat{U}_{\mathbf{p}}=p^{2}/(2m)+\hat{\sigma}_{z}w_{\mathbf{p}}, \tag{A4}$$

and consequently a linear p-dependent contribution appears in the dispersion law $\varepsilon_{\sigma\mathbf{p}}$ if $\mathbf{H}=0$, while a nonsymmetric dispersion law appears for the in-plane magnetic field.

An explicit expression for vector $\mathbf{u}_{\mathbf{p}}$ is obtained from the system of equations:

$$(\mathbf{u}_{\mathbf{p}}\cdot\mathbf{u}_{\mathbf{p}})=1,\quad(\mathbf{w}_{\mathbf{p}}\cdot\mathbf{u}_{\mathbf{p}})=0. \tag{A5}$$

The orthogonality condition thus yields

$$\mathbf{u}_{\mathbf{p}}=\mathcal{N}\left\{[\mathbf{p}\times\mathbf{v}_{s}]+\mathbf{p}\frac{(\mathbf{v}_{s}\cdot[\mathbf{p}\times\mathbf{w}_{\mathbf{p}}])}{(\mathbf{p}\cdot\mathbf{w}_{\mathbf{p}})}\right\}, \tag{A6}$$

where the normalization constant $\mathcal{N}$, is equal to $(\mathbf{p}\cdot w_{\mathbf{p}})/(w_{\mathbf{p}}v_s p^2)$. The final result for the solution of Eq. (A5) is

$$\mathbf{u_p}=[\mathbf{w_p}\times\mathbf{v}_s]/(w_{\mathbf{p}}v_s), \tag{A7}$$

and this expression has been used in Eq. (2).

It is convenient to introduce the vector $\mathbf{e}\equiv[\mathbf{v}_s\times\mathbf{E}]$ in order to obtain the matrix elements for the spin-flip transitions used in the generation term $\delta G^{(eq)}_{\sigma\mathbf{p}}$ [see Eqs. (7) and (9)]. The general expression for such a matrix element may be written as

$$\begin{aligned}|\langle +1\mathbf{p}|(\hat{\boldsymbol{\sigma}}\cdot\mathbf{e})|-1\mathbf{p}'\rangle|^2\\ &=\frac{1}{4}|\langle +1|\{1-i(\hat{\boldsymbol{\sigma}}\cdot\mathbf{u_p})\}(\hat{\boldsymbol{\sigma}}\cdot\mathbf{e})\{1+i(\hat{\boldsymbol{\sigma}}\cdot\mathbf{u_{p'}})\}|-1\rangle|^2\\ &=\frac{1}{4}|(e_x-ie_y)[1-(\mathbf{u_p}\cdot\mathbf{u_{p'}})]\\ &\quad+(\mathbf{u_p}\cdot\mathbf{e})(u^x_{\mathbf{p}'}-iu^y_{\mathbf{p}'})+(\mathbf{u_{p'}}\cdot\mathbf{e})(a^x_{\mathbf{p}}+iu^y_{\mathbf{p}})|^2.\end{aligned} \tag{A8}$$

Taking into account

$$(\mathbf{u_p}\cdot\mathbf{u_{p'}})=\frac{\mathbf{w_p}\cdot\mathbf{w_{p'}}}{w_{\mathbf{p}}w_{\mathbf{p}'}},\quad (\mathbf{u_p}\cdot\mathbf{e})=\frac{\mathbf{v}_s}{w_{\mathbf{p}}}(\mathbf{E}\cdot\mathbf{w_p}), \tag{A9}$$

we transform (A8) into

$$\begin{aligned}|\langle +1\mathbf{p}|(\hat{\boldsymbol{\sigma}}\cdot\mathbf{e})|-1\mathbf{p}'\rangle|^2\\ &=\frac{1}{4}\Bigg|(E_x-iE_y)\left[\frac{(\mathbf{w_p}\cdot\mathbf{w_{p'}})}{w_{\mathbf{p}}w_{\mathbf{p}'}}-1\right]+\frac{v_s(\mathbf{E}\cdot\mathbf{w_p})}{w_{\mathbf{p}}}\,\frac{w^x_{\mathbf{p}'}-iw^y_{\mathbf{p}'}}{w_{\mathbf{p}'}}\\ &\quad+\frac{v_s(\mathbf{E}\cdot\mathbf{w_{p'}})}{w_{\mathbf{p}'}}\,\frac{w^x_{\mathbf{p}}-iw^y_{\mathbf{p}}}{w_{\mathbf{p}}}\Bigg|^2\end{aligned} \tag{A10}$$

and for coinciding 2D momenta $\mathbf{p}=\mathbf{p}'$ this matrix element takes a simple form $v_s^2(\mathbf{E}\cdot\mathbf{w})^2/4$. Linearized in $\hbar\mathbf{q}$ the contributions to these matrix element (such linearization is denoted by an overline below) may be obtained after straightforward algebraic transformations

$$\begin{aligned}\overline{|\langle +1,\mathbf{p}+\hbar\mathbf{q}|(\hat{\boldsymbol{\sigma}}\cdot\mathbf{e})|-1,\mathbf{p}\rangle|^2}&=-\overline{|\langle +1,\mathbf{p}|(\hat{\boldsymbol{\sigma}}\cdot\mathbf{e})|-1,\mathbf{p}-\hbar\mathbf{q}\rangle|^2}\\ &=\frac{v_s^2}{w_{\mathbf{p}}}(\mathbf{E}\cdot\mathbf{w_p})(\mathbf{E}\cdot[\mathbf{v}_s\times\hbar\mathbf{q}]),\end{aligned} \tag{A11}$$

and this value has been used in Eqs. (12) and (13) for the PD current.

APPENDIX B

The consideration of quantum correction to the PD current $\delta\mathbf{J}$, which is due to the multiplication of high-frequency contributions to the density matrix and proportional to the $\exp(i\mathbf{qx}-i\omega t)$ terms in the current operator, is given below. The general expression for the current density operator at the point $\mathbf{X}$ may be written as a variational derivative of the Hamiltonian (1) with respect to the vector potential:

$$\hat{\mathbf{J}}_{\mathbf{X}}+\left(i\frac{e^2}{m\omega}\mathbf{E}e^{i\mathbf{qx}-i\omega t}\delta(\mathbf{x}-\mathbf{X})+\text{h.c.}\right), \tag{B1}$$

where the steady-state part of the current operator $\hat{\mathbf{J}}_{\mathbf{X}}$ takes the form

$$\begin{aligned}\hat{\mathbf{J}}_{\mathbf{X}}=&\frac{e}{2m}[\hat{\mathbf{p}}\delta(\mathbf{x}-\mathbf{X})+\delta(\mathbf{x}-\mathbf{X})\hat{\mathbf{p}}]+e[\boldsymbol{\sigma}\times\mathbf{v}_s]\delta(\mathbf{x}-\mathbf{X})\\ &+ig\frac{|e|}{2m_e}\{[\hat{\mathbf{p}}\times\hat{\boldsymbol{\sigma}}]\delta(\mathbf{x}-\mathbf{X})+\delta(\mathbf{x}-\mathbf{X})[\hat{\mathbf{p}}\times\hat{\boldsymbol{\sigma}}]\}.\end{aligned} \tag{B2}$$

Here m_e is the free-electron mass and $\mathbf{x}$ and $\hat{\mathbf{p}}$ obey the usual commutation relation $[x_i,\hat{p}_j]_-=i\delta_{ij}\hbar$. This current operator leads to the velocity operator $\mathbf{p}/m+[\hat{\boldsymbol{\sigma}}\times\mathbf{v}_s]$ if only the homogeneous PD currents and zero-wave-vector Fourier components in Eq. (B1) are essential.

Quantum corrections to the PD current appear due to the second addendum in Eq. (B1) and such a contribution to Eq. (3) is presented as

$$\delta\mathbf{J}_{\mathbf{X}}=i\frac{e^2\mathbf{E}}{m\omega}\int_{-\pi/\omega}^{\pi/\omega}dt\,sp\,\delta(\mathbf{x}-\mathbf{X})\,\delta\hat{\rho}_t e^{i\mathbf{qx}-i\omega t}, \tag{B3}$$

where $\delta\hat{\rho}_t$ describes the linear response due to the perturbation (5). This may be written as

$$\delta\hat{\rho}_t=\frac{e^{-i\omega t}}{i\hbar}\int_{-\infty}^{0}d\tau e^{\lambda\tau}e^{(i/\hbar)\hat{h}\tau}[\delta\hat{h}e^{-i\omega t},\hat{\overline{\rho}}]_-e^{-(i/\hbar)\hat{h}\tau}+\text{H.c.} \tag{B4}$$

After substitution of Eq. (B4) into Eq. (B3) we obtain

$$\begin{aligned}\delta\mathbf{J}_{\mathbf{X}}&=\frac{e^2/m}{\hbar\omega}\mathbf{E}e^{-i\mathbf{qX}}sp\,\delta(\mathbf{x}-\mathbf{X})\int_{-\infty}^{0}d\tau e^{\lambda\tau-i\omega\tau}e^{(i/\hbar)\hat{h}\tau}[\delta\hat{h},\hat{\overline{\rho}}]_-e^{-(i/\hbar)\hat{h}\tau}+\text{c.c.}\\ &=\frac{e^2/m}{\hbar\omega}\,\frac{\mathbf{E}}{L^2}\sum_{\sigma\mathbf{p}}\int_{-\infty}^{0}d\tau e^{\lambda\tau-i\omega\tau}\langle\sigma\mathbf{p}|\delta\hat{h}|\sigma\mathbf{p}\rangle(f_{\sigma\mathbf{p}}-f_{\sigma\mathbf{p}+\hbar\mathbf{q}})+\text{c.c.}\end{aligned} \tag{B5}$$

using also the basis (2) in the last expression.

In the first-order approximation in $\hbar\mathbf{q}$ we use a matrix element $\langle\sigma\mathbf{p}|\delta\hat{h}|\sigma\mathbf{p}\rangle\sim(\mathbf{E}\cdot\mathbf{p})$ and the expression for $\delta\mathbf{J}$ hence transforms as

$$\delta\mathbf{J}\simeq\frac{e^2/m}{\hbar\omega}\mathbf{E}\sum_\sigma\int\frac{d\mathbf{p}}{(2\pi\hbar)^2}\left(\frac{i}{\omega+i\lambda}\right)\left(-i\frac{e\mathbf{E}\cdot\mathbf{p}}{m\omega}\right)\left(\hbar\mathbf{q}\frac{\partial f\sigma_\mathbf{p}}{\partial\mathbf{p}}\right)+\text{c.c.}=\frac{2ne^2\mathbf{E}}{m\hbar\omega^2}\left(\frac{e\mathbf{E}\cdot\hbar\mathbf{q}}{m\omega}\right). \tag{B6}$$

By this means, instead of the characteristic velocity v_{PD}, which is determined by Eq. (21) we have obtained here a velocity of the order of $(eE/\omega)^2\sqrt{\epsilon}/(m^2c)$ and such a contribution is less than v_{PD} by the factor $(\omega\overline{\tau})^2mv_s^3/(\Gamma v_F)$. This factor is equal approximately to 4×10^{-4} for the numerical parameters used above.

[1] A. D. Wieck, H. Sigg, and K. Ploog, Phys. Rev. Lett. **64**, 463 (1990); H. Sigg, P. van Son, and K. Kohler, Surf. Sci. **361/362**, 468 (1996).

[2] O. Keller, Phys. Rep. **268**, 86 (1996).

[3] R. Kesselring, A. W. Kalin, H. Siggs, and F. K.Kneubuhl, Rev. Sci. Instrum. **63**, 3317 (1992).

[4] M. S. Sherwin, K. Craig, B. Galdrikian, J. Heyman, A. Markelz, K. Campman, S. Fafard, P. F. Hopkins, and A. Gossard, Physica D **83**, 229 (1995); J. N. Heyman, K. Craig, B. Galdrikian, M. S. Sherwin, K. Campman, P. F. Hopkins, S. Fafard, and A. C. Gossard, Phys. Rev. Lett. **72**, 2183 (1994).

[5] F. T. Vasko, Phys. Rev. B **53**, 9576 (1996).

[6] X. Chen and O. Keller, Phys. Rev. B **55**, 15 706 (1997).

[7] F. J. Ohkawa and Y. Uemura, J. Phys. Soc. Jpn. **37**, 1325 (1974); Y. Takada, K. Arai, N. Uchimura, and Y. Uemura, *ibid.* **49**, 1851 (1980).

[8] F. T. Vasko, Pisma Zh. Eksp. Teor. Fiz. **30**, 574 (1979) [JETP Lett. **30**, 541 (1979); Fiz. Tech. Poluprovodn. **19**, 1958 (1985) [Sov. Phys. Semicond. **19**, 1207 (1985)].

[9] Ya. A. Buchkov, E. I. Rashba, Pisma Zh. Eksp. Teor. Fiz. **39**, 66 (1984) [JETP Lett. **39**, 78 (1984)]; J. Phys. C **17**, 6039 (1984).

[10] B. Das, D. C. Miller, S. Datta, R. Reifenberger, W. P. Hong, P. K. Bhattacharya, J. Singh, and M. Jaffe, Phys. Rev. B **39**, 1411 (1989).

[11] J. Luo, H. Munekata, F. F. Fang, and P. J. Stiles, Phys. Rev. B **41**, 7685 (1990).

[12] J. P. Heida, B. J. van Wees, T. M. Klapwijk, G. Borghs, in *Proceedings of the 23rd International Conference on the Physics of Semiconductors*, edited by M. Scheffler and R. Zimmermann (World Scientific, Singapore, 1996), p. 246.

[13] J. Nitta, T. Akazaki, H. Takayanagi, and T. Enoki, Phys. Rev. Lett. **78**, 1335 (1997).

[14] B. Jusserand, D. Richards, G. Allan, C. Priester, and B. Etienne, Phys. Rev. B **51**, 4707 (1995).

[15] R. Winkler and U. Rossler, Phys. Rev. B **48**, 8918 (1993).

[16] E. A. de Andrada e Silva, G. C. La Rocca, and F. Bassani, Phys. Rev. B **55**, 16 293 (1996).

[17] F. T. Vasko, Fiz. Tech. Poluprovodn. **18**, 86 (1984) [Sov. Phys. Semicond. **18**, 51 (1984)].

[18] F. T. Vasko and O. Keller, Phys. Status Solidi B **204**, 39 (1997).

[19] F. T. Vasko and N. A. Prima, Fiz. Fverd. Tela **25**, 582 (1983) [Sov. Phys. Solid State **25**, 331 (1983)].

[20] V. M. Edelshtein, Zh. Exp. Teor. Fiz. **94**, 264 (1988).

[21] L. I. Magarill, Fiz. Tverd. Tela (Leningrad) **32** (1990) [Sov. Phys. Solid State **32** (1990)].

[22] F. T. Vasko, Fiz. Techn. Poluprovodn. **19**, 1319 (1985) [Sov. Phys. Semicond. **19**, 808 (1985)].

[23] S. Luryi, Phys. Rev. Lett. **58**, 2263 (1987); A. A. Grinberg and S. Luryi, Phys. Rev. B **38**, 87 (1988).

[24] L. E. Gurevich and A. Ya. Vinnikov, Fiz. Tverd. Tela **15**, 87 (1973) [Sov. Phys. Solid State **15**, 58 (1973)].

[25] According to T. P. Smith and F. F. Fang [Phys. Rev. B **35**, 7729 (1987)] $|g|$ for 2D electrons in a narrow InAS well decreases in comparison with the bulk value [see C. R. Pidgeon, D. L. Mitchell, and R. N. Brown, Phys. Rev. **154**, 737 (1967)].